ASTRONOMY & ASTROPHYSICS
SUPPLEMENT SERIES

Astron. Astrophys. Suppl. Ser. **137**, 147–156 (1999)

A representative sample of Be stars

I. Sample selection, spectral classification and rotational velocities

I.A. Steele[1], **I. Negueruela**[1,2], **and J.S. Clark**[3]

[1] Astrophysics Research Institute, Liverpool John Moores University, Twelve Quays House, Egerton Wharf, Birkenhead, L41 1LD, UK
[2] SAX SDC, Italian Space Agency, c/o Telespazio, via Corcolle 19, I-00131 Rome, Italy
[3] Astronomy Centre, CPES, University of Sussex, Brighton BN1 9QH, UK

Received September 7, 1998; accepted March 12, 1999

Abstract. We present a sample of 58 Be stars containing objects of spectral types O9 to B8.5 and luminosity classes III to V. We have obtained $3670 - 5070$ Å spectra of the sample which are used to derive spectral types and rotational velocities. We discuss the distribution of spectral types and rotational velocities obtained and conclude that there are no significant selection effects in our sample.

Key words: stars: emission-line, Be — stars: fundamental parameters — stars: rotation

1. Introduction

Fundamental questions still outstanding with regard to Be stars are the radial dependence of the density, temperature and velocity structure of the circumstellar disk surrounding the star. In addition the dependence of these parameters on the effective temperature (spectral type), evolutionary status (luminosity class), and rotational velocity of the underlying B star is unknown. In an attempt to answer these questions we have devised a multiwavelength approach which combines optical and infrared spectroscopy of a carefully selected sample of Be stars containing both giants and dwarfs of spectral types from O9 to B8.5. Our dataset comprises observations of 58 Be stars in 5 wavelength regions and is summarised in Table 1.

This paper presents the details of the sample selection and an analysis of the classification (absorption line) features in the $3670 - 5070$ Å spectra. We defer discussion of the emission line features in these spectra to subsequent papers, where we will consider them in conjunction with the emission line spectra at other wavelengths.

Send offprint requests to: I.A. Steele
Correspondence to: ias@astro.livjm.ac.uk

2. Sample selection

A Be star is defined as a B-type non-supergiant star that shows, or has shown in the past, emission lines. Jaschek & Egret (1982) provide a list of such objects, and it is from that list our sample is drawn. We note here that as the Be phenomenon is time variable we expect several of our objects not to show emission lines at present.

Our sample is termed a "representative" sample, in that it was selected in an attempt to contain several objects that were typical of each spectral and luminosity class for which the Be phenomenon occurs. It therefore does *not* reflect the spectral and luminosity class space distribution of Be stars, but only the attempts to define the average properties of each subclass in temperature and luminosity. Our selection was made according to the following criteria:

1. An equal distribution of spectral types from B0 to B9 using the spectral types listed by Jaschek & Egret (1982).
2. An equal distribution between dwarf and giant luminosity classes listed by Jaschek & Egret (1982).
3. No evidence of spectroscopic binarity in the literature.

The following additional constraints were imposed by the instrument sensitivity and time allocation:

1. Right Ascensions in the range $17^{\rm h}$ to $6^{\rm h}$.
2. Declinations in the range to $+59^\circ > \delta > -27^\circ$.
3. B magnitude brighter than $\sim$11.

These criteria were designed in an attempt to create a sample containing roughly 3 objects per spectral type per luminosity class. We note here that no selection criteria

Table 1. Summary of observations of the sample

Wavelength Range (Å)	Resolution (km s^{-1})	Date Obtained	Emission Lines Seen
3670 − 5070	∼55	1998 Aug.	Hβ - H limit, HeI, Mg II, Fe II
5850 − 7150	∼35	1998 Aug.	Hα, He I
7800 − 9200	∼30	1998 Aug.	Paschen 6 – Paschen limit, He I
15300 − 16900	∼100	1996 Jun. + Oct.	Brackett 11 to 18
20550 − 22100	∼70	1996 Jun. + Oct.	Mg II, He I, Br γ, Fe II, Na I

Table 2. Data on the sample from the SIMBAD database (Coordinates J2000)

OBJECT	RA	DEC	B	V	Alias	Historical Spectral Type(s)
CD −28 14778	18 37 40.0	−27 59 07	9.06	8.95	HD 171757	B2nne, B3IIIe
CD −27 11872	17 44 45.7	−27 13 44	9.13	8.69	V3892 Sgr, HD 161103	Be, B2:IVpe, B2III-IVpe
CD −27 16010	22 40 39.2	−27 02 37	4.06	4.20	ϵ PsA, HR 8628, HD 214748	B8V, B7, B8Ve
CD −25 12642	18 03 44.0	−25 18 54	9.29	9.00	HD 164741	B2Ib/II, B1III
CD −22 13183	18 39 30.1	−21 57 56	8.08	7.90	HD 172158	B8II
BD −20 05381	19 03 33.1	−20 07 42	7.76	7.80	HD 177015	B4Vn, B5III
BD −19 05036	18 31 24.1	−19 09 31	8.26	7.92	V3508 Sgr, HD 170682	B5II/III, B7III
BD −12 05132	18 39 39.7	−11 52 43	10.13	9.48	HD 172252	B0Ve, B2Vnpe
BD −02 05328	20 39 13.1	−02 24 46	6.12	6.22	HD 196712	B7IIIne B8Ve
BD −01 03834	19 49 33.4	−01 06 03	8.25	8.14	HD 187350	B1Vne
BD −00 03543	18 44 55.8	−00 22 23	6.87	6.88	HD 173371	B9III
BD +02 03815	19 12 03.2	+02 37 22	7.03	6.92	HD 179343	B9
BD +05 03704	18 21 28.4	+05 26 09	6.09	6.13	HD 168797	B3Ve, B2Ve
BD +17 04087	19 46 57.8	+18 14 56	10.6	10.6	HD 350559	B7IIIe
BD +19 00578	03 42 18.9	+19 42 02	5.68	5.69	13 Tau, HR 1126, HD 23016	B9Vn, B8Ve
BD +20 04449	20 09 39.6	+21 04 44	8.3	8.3	HD 191531	B0.5 III-V
BD +21 04695	22 07 50.4	+21 42 14	5.68	5.78	25 Peg, HD 210129	B7Vn, B6V, B8V
BD +23 01148	06 01 05.8	+23 20 20	7.97	7.36	HD 250289	B2IIIe
BD +25 04083	20 04 00.7	+26 16 17	9.57	8.94	HD 339483	B1III
BD +27 00797	05 34 36.6	+27 35 34	10.31	9.86	HD 244894	B1III-IVpe
BD +27 00850	05 44 27.7	+27 13 48	9.54	9.38	HD 246878	B0.5Vpe
BD +27 03411	19 30 45.3	+27 57 55	5.01	5.15	β2 Cyg, HR 7418, HD 183914	B8V, B7V
BD +28 03598	20 03 11.7	+28 42 27	10.45	9.43	HD 333452	B0III:np
BD +29 03842	20 00 33.5	+30 22 52	10.60	10.11	HD 33226	B1Ve
BD +29 04453	21 35 44.4	+29 44 44	8.15	8.10	HD 205618	B2Vne
BD +30 03227	18 33 23.0	+30 53 32	6.47	6.58	HR 6971, HD 171406	B4V, B3Vn
BD +31 04018	20 16 48.2	+32 22 48	7.25	7.16	V2113 Cyg, HD 193009	B1V:nnpe
BD +36 03946	20 13 50.2	+36 37 23	9.0	9.2	HD 228438	B0.5III, B0IV
BD +37 00675	03 00 11.7	+38 07 55	6.05	6.16	HR 894, HD 18552	B8Vn, B8Ve, B9V
BD +37 03856	20 16 08.4	+37 33 23	10.58	10.20	HD 228650	B1V
BD +40 01213	05 13 13.3	+40 11 37	7.38	7.34	HD 33604	B2Vpe
BD +42 01376	05 42 19.9	+43 03 35	7.27	7.28	V434 Aur, HD 37657	B3Vne
BD +42 04538	22 55 47.0	+43 33 34	8.06	8.02	HD 216581	B3Vn
BD +43 01048	04 45 51.4	+43 59 40	9.81	9.53	HD 276738	B7V
BD +45 00933	04 25 49.9	+46 14 02	8.38	8.06	HD 27846	B1.5V
BD +45 03879	22 19 00.2	+45 48 08	8.48	8.48	HD 211835	B3Ve, B2n
BD +46 00275	01 09 30.1	+47 14 31	4.18	4.25	ϕ And, HR 335, HD 6811	B7III, B7IV, B7V, B8III
BD +47 00183	00 44 43.4	+48 17 04	4.47	4.50	22 Cas, HR 193, HD 4180	B5III, B2V, B3IV, B2Ve
BD +47 00857	03 36 29.2	+48 11 35	4.17	4.23	ψ Per, HR 1087, HD 22192	B5Ve, B5ne, B5IIIe, B5V
BD +47 00939	04 08 39.5	+47 42 47	4.01	4.04	48 Per, HR 1273, HD 25940	B3Ve, B3p, B3Vpe
BD +47 03985	22 57 04.4	+48 41 03	5.33	5.42	EW Lac, HR 8731, HD 217050	B3IVpe, B2pe, B5ne
BD +49 00614	02 16 36.0	+49 49 12	7.59	7.57	HD 13867	B5Ve, B8e
BD +50 00825	03 48 18.2	+50 44 12	6.20	6.15	HR 1160, HD 23552	B8Vn, B7V
BD +50 03430	21 46 02.7	+50 40 27	6.96	7.02	HD 207232	B9
BD +51 03091	21 34 27.4	+51 41 54	6.17	6.19	HR 8259, HD 20551	B9III
BD +53 02599	21 19 44.8	+53 57 06	8.34	8.08	HD 203356	B9
BD +55 00552	02 15 02.5	+55 47 36	8.25	7.90	HD 13669	B3IV-V, B2Vne, B2V
BD +55 00605	02 23 35.4	+56 34 28	9.61	9.34	V361 Per, HD 14605	B0.5Vpe, B1.5IIIe
BD +55 02411	20 29 27.0	+56 04 06	5.87	5.89	HD 195554	B9Vn
BD +56 00473	02 16 57.6	+57 07 49	9.33	9.08	V356 Per	B0.5IIIn, B1III, B1II, B3e
BD +56 00478	02 17 08.1	+56 46 11	8.70	8.51	V358 Per, HD 13890	B1III, B1IIIpe, B3e
BD +56 00484	02 17 44.6	+56 54 00	9.94	9.62	V502 Per	B1IIIe, B0Vne, B0ne
BD +56 00493	02 18 18.0	+56 51 03	9.81	9.62	-	B1Vpe
BD +56 00511	02 18 47.9	+57 04 02	9.49	9.11	-	B3III
BD +56 00573	02 22 06.4	+57 05 25	10.06	9.66	-	B2III - IVe
BD +57 00681	03 02 37.8	+57 36 46	9.34	8.66	HD 237056	B0.5Bpe, 08ne
BD +58 00554	03 04 30.5	+59 26 47	9.49	9.16	HD 237060	B9V
BD +58 02320	21 44 33.9	+59 03 26	9.77	9.51	HD 239758	B2III:nn, B2Vn(e)

was applied for $v \sin i$, as the distribution of $v \sin i$ with spectral type and luminosity class was one of the phenomena we wished to investigate. The achieved spectral and luminosity class distribution is somewhat different to the 3 per spectral type per luminosity class, with many more dwarfs than giants in the sample. This is not surprising given that Jaschek & Egret (1982) is simply a compilation of values from the literature, with most of the spectral types from low resolution photographic spectra taken in the 1950's. The achieved distribution is discussed in Sects. 4 and 5, along with a discussion of possible biases in the sample.

There are a total of 58 objects in our sample. In Table 2 we list the sample by BD number, along with other aliases for the brighter/well studied objects. Also listed in Table 2 are J2000 coordinates and B and V magnitudes for the sample from the SIMBAD database, and the historical spectral types assigned to the objects.

Note that there is a large variation in the historical spectral types, with many objects having a spectral class uncertain by 2 sub-types and a similarly uncertain luminosity class. We assume this is due to the quality of the spectra used. Although Be stars show great time variability in their emission line spectra, we are aware of no evidence in the modern literature to indicate variability of the underlying B star absorption spectrum. Since the overall aim of this programme is to understand the relationship between the parameters of underlying stars and the circumstellar disks in these systems it is therefore necessary to reclassify all of the stars in our sample using modern CCD spectra. This need to reclassify the sample is the motivation for the observations presented here.

Table 3. Spectral standards observed (* = see text)

HD Number	Alias	Spectral Type
HD 214680	10 Lac	O9V
HD 34078	AE Aur	O9.5V
HD 209975	19 Cep	O9.5Ib
HD 149438	τ Sco	B0.2V
HD 22951	40 Per	B0.5V
HD 218376	1 Cas	B0.5III
HD 144470	ω^1 Sco	B1V
HD 23180	o Per	B1III
HD 243980	ζ Per	BI1b
HD 214993	12 Lac	B1.5III
HD 148605	22 Sco	B2V
HD 886	γ Peg	B2IV
HD 29248	ν Eri	B2III
HD 207330	π^2 Cyg	B2.5III
HD 198478	55 Cyg	B2.5Ia
HD 20365	29 Per	B3V
HD 160762	ι Her	B3IV
HD 219688	ψ^2 Aqr	B5V
HD 147394	τ Her	B5IV
HD 184930	ι Aql	B5III
HD 23338	19 Tau	B6V*
HD 23302	17 Tau	B6III*
HD 23288	16 Tau	B7IV
HD 23630	η Tau	B7III
HD 214923	ζ Peg	B8V*
HD 23850	27 Tau	B8III
HD 196867	α Del	B9V*
HD 176437	γ Lyr	B9III
HD 222661	ω^2 Aqr	B9.5V
HD 186882	δ Cyg	B9.5III

3. Observations

The classification spectra were obtained using the IDS spectrograph of the Isaac Newton Telescope, La Palma on the night of 1998 August 2. The R1200B grating was employed with a slit width of 1.15 arcsec and the EEV12 CCD. This gives a dispersion of ~ 0.5 Å/pixel. A central wavelength was chosen of 4300 Å, giving a a wavelength range of $3670 - 5070$ Å. Measurements of interstellar features in the spectra give a full width half maximum corresponding to a velocity resolution of ~ 55 km s^{-1}. In addition to our Be star sample we obtained spectra of 30 MK standards in the range O9 to B9.5, mainly of luminosity classes III and V (Table 3).

4. Spectral classification

4.1. General methodology

The observed spectrum of Be stars is a composite of the photospheric absorption spectrum and the spectrum produced by the envelope, i.e., an additional continuum component on which emission and absorption lines can be superimposed. For most Be stars, the contribution of the envelope to the continuum in the classical "classification region" ($\lambda\lambda$ 3900 – 4900 Å) is not very important (Dachs et al. 1989). However, the envelope can still contribute emission in the lines of H I, He I and several metallic ions. Weak emission can result in the "in-filling" of photospheric lines, while stronger emission results in the appearance of emission lines well above the continuum level. With sufficient spectral resolution and a high enough $v \sin i$ the emission lines appear double peaked. A well-developed "shell" spectrum, with a large number of metallic absorption lines can completely veil the photospheric absorption spectrum (see the spectrum of BD +02°3815 in Fig. 3).

Since the relative strengths of several He I lines intervene in most classification criteria for the MK system in the spectral range of interest, the spectral classification of Be stars has always been considered particularly complicated. In many spectra, the in-filling of He I lines affects the main classification criteria. When Fe II emission is present, several lines which are used as classification criteria can be veiled (such as the Si II $\lambda\lambda$ 4128 – 4130 Å doublet).

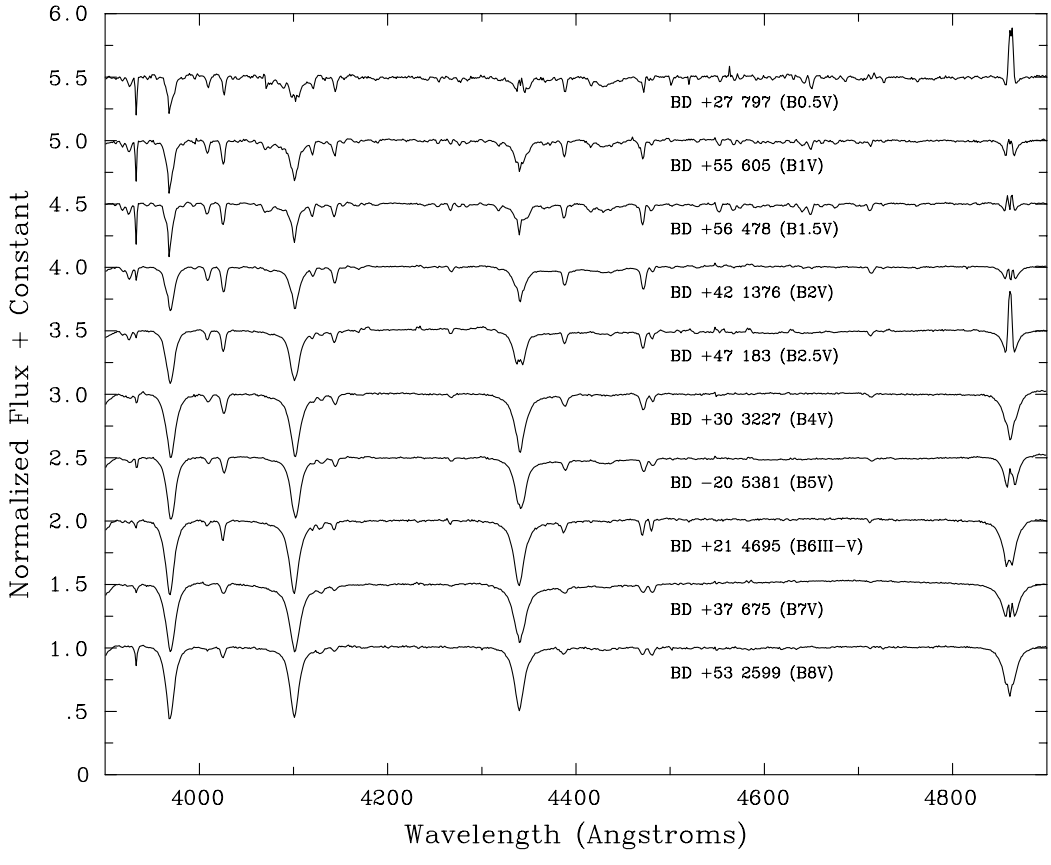

Fig. 1. Spectral sequence for main sequence stars. Note the progressive decline of the He I spectrum from a maximum at B1−B2 and the increase of Mg II λ4481 Å with spectral type. We note that the spectrum of BD +37 675 shows Mg II λ4481 Å $\simeq$ He I λ4471 Å, which defines B8. However, since He I $\lambda\lambda$4711, 4009, 4121 Å and C II λ4267 Å are still visible, we have preferred a B7V spectral type, assuming that He I λ4471 Å is partially filled-in. If this is not the case, an intermediate spectral type (B7.5V) would seem necessary

The high resolutions obtainable at high signal-to-noise ratio with modern CCD cameras improve the situation, since they allow us to disentangle lines that were blended at the resolutions formerly used for spectral classification. On the other hand, the improved resolution means that the traditional criteria are not always applicable. Our spectra have a much higher resolution than the 63 Å mm^{-1} plates used by Walborn (1971) to define the grid for early-type B stars. Given that the only acceptable methodological procedure in the MK scheme is the comparison of spectra (Morgan & Keenan 1973), all this results in a strong dependence on the choice of standard stars. Unfortunately, the standard stars available for observation are limited by the position of the observatory and time of the year. Our standard stars, taken from the lists of Walborn (1973) and Jaschek & Gómez (1998) are listed in Table 3. We point out that Jaschek & Gómez (1998) give HD 23338 (19 Tau) as a B6V standard and HD 196867 (α Del) as B9V, while Morgan & Keenan (1973) give them as B6IV and B9IV respectively. At our resolution, neither of the two spectra can be justifiably classified as main sequence objects and we endorse the subgiant classification. Indeed HD 23338 looks remarkably similar to HD 23302 (17 Tau), which is given by Jaschek & Gómez (1998) and Lesh (1968) as the primary B6III standard.

For classification purposes, we compared the spectra of the Be stars with those of the standard stars in the interval $\lambda\lambda$ 3940 − 4750 Å both at full instrumental resolution and binned to 1.2 Å/pixel to mimic the resolution of photographic plates. The comparison was done both "by eye" and using the measured equivalent widths of the relevant features. All the spectra have been classified in this scheme without previous knowledge of spectral classifications existent in the literature. The derived spectral types are listed in Table 4. Representative spectral and luminosity sequences are shown in Figs. 1 and 2, and some peculiar spectra from the sample are shown in Fig. 3.

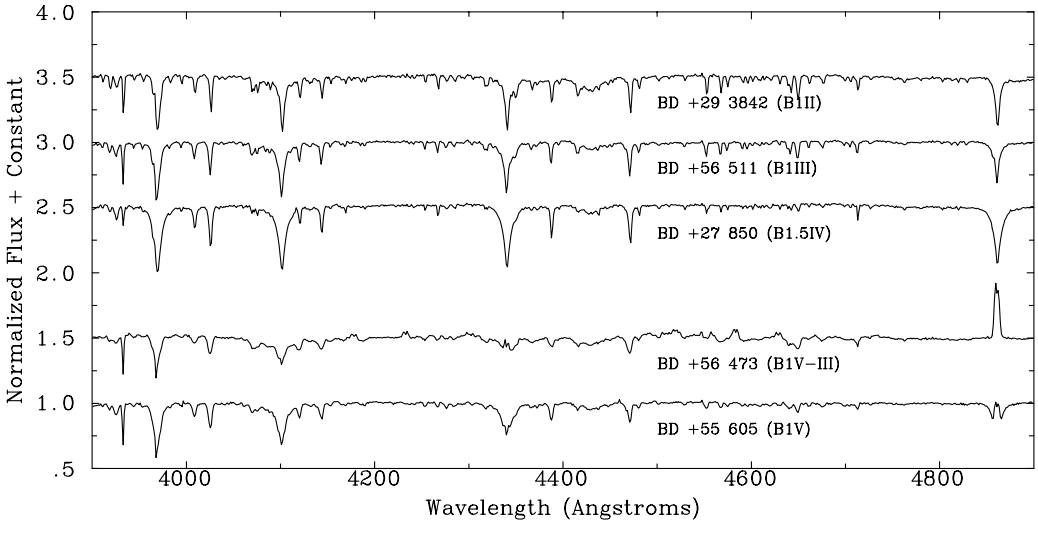

Fig. 2. Luminosity Sequence near B1. Note the increase in the metallic (mainly O II) spectrum with luminosity class, not so obvious in BD +27 850 because of the later spectral type. The emission veiling in BD +56 473 is too strong to allow an exact classification, even though the strong O II + C III near λ4650 Å seems to favour the giant classification

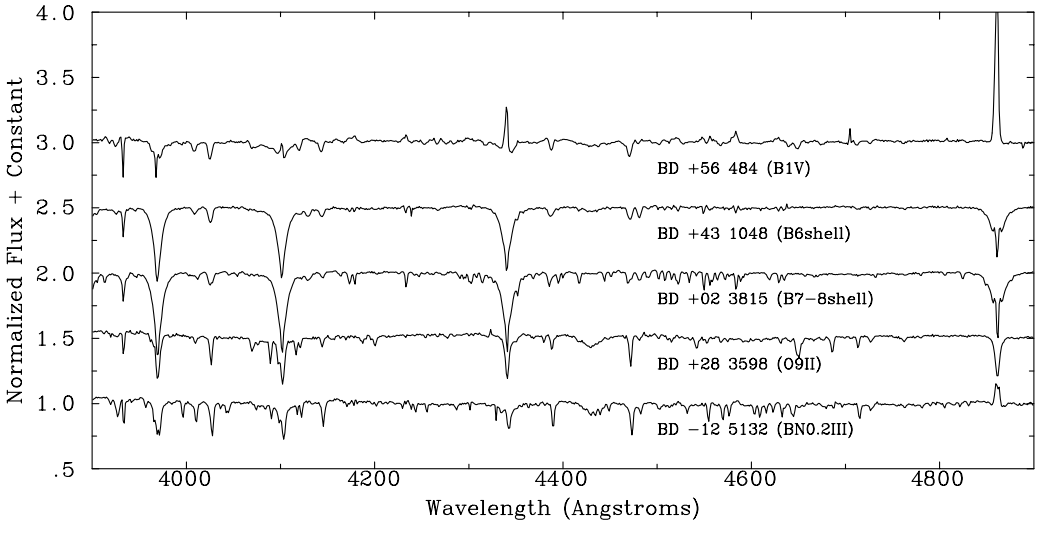

Fig. 3. Some peculiar spectra in our sample. BD +56°484 (B1Ve) has a very strong emission spectrum, with abundant Fe II features. For late types, Fe II is only seen in shell spectra, like that of BD +43°1048 (B6IIIshell). BD +02°3815 (B7-8shell) shows a fully developed shell spectrum. The earliest spectrum in our sample is that of BD +28°3598 (O9II), where no evidence of emission is detectable. Finally, BD −12°5132 (BN0.2IIIe) is N-enhanced, showing strong N II $\lambda\lambda$ 3995, 4044, 4242, 4631 Å among others, while C II $\lambda\lambda$ 4076, 4650 Å are absent

We find that the accuracy that can be obtained in the classification depends in part on the spectral type of the object, as described below.

4.2. Early B stars

For stars earlier than B3, the classification can be adequately performed using as main indicators the Si IV and Si III lines. The strength of these lines and of the O II spectrum is very sensitive to temperature and luminosity variations. Moreover, the emission spectrum does not generally extend shortwards of $\sim \lambda$4200 Å. As a consequence, most of our determinations in this spectral range are very secure. Even though the spectral grid is finer than at later types, we believe that most objects are correctly classified to the sub-subtype, i.e., a spectrum classified as B0.7III is

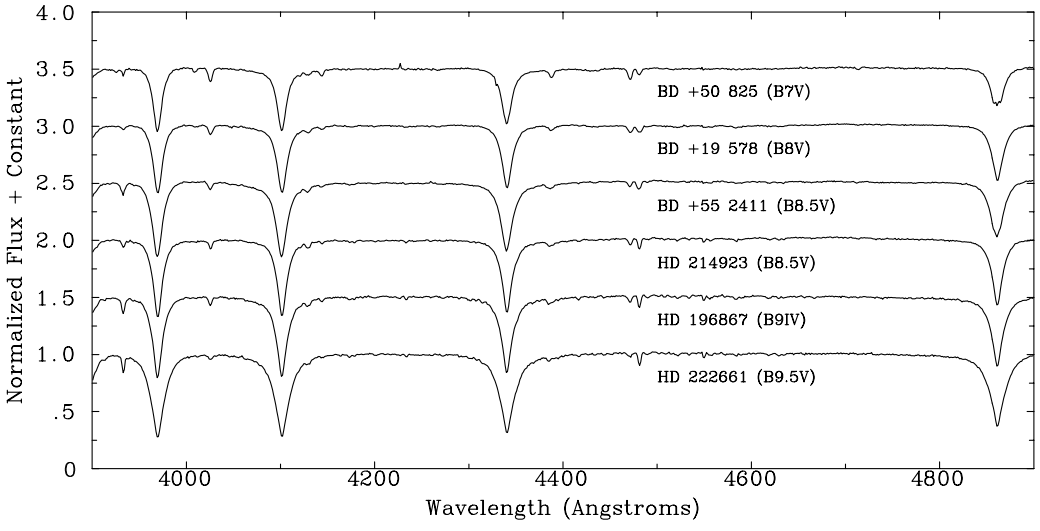

Fig. 4. Spectral sequence for late B-type stars. In BD +50°825 (B7Ve), He I λ4471 Å is still stronger than Mg II λ4481 Å, but in BD +19°578, the two lines have about the same strength, making the object B8V. He I $\lambda\lambda$ 4009, 4121 Å are not visible in this spectrum. Both BD +55°2411 and HD 214923 have Mg II λ4481 Å stronger than He I λ4471 Å, which makes them later, even though HD 214923 is given as B8V standard. Comparison of HD 214923 with HD 196867 (B9IV) and HD 222661 (B9.5V) shows that it is not later than B9V. BD +55°2411 is earlier than HD 214923, since it shows stronger He I $\lambda\lambda$ 4026, 4387 Å and no sign of Fe II absorption. Therefore a spectral type B8.5V seems justified. This spectrum shows no sign of emission over the whole classification range

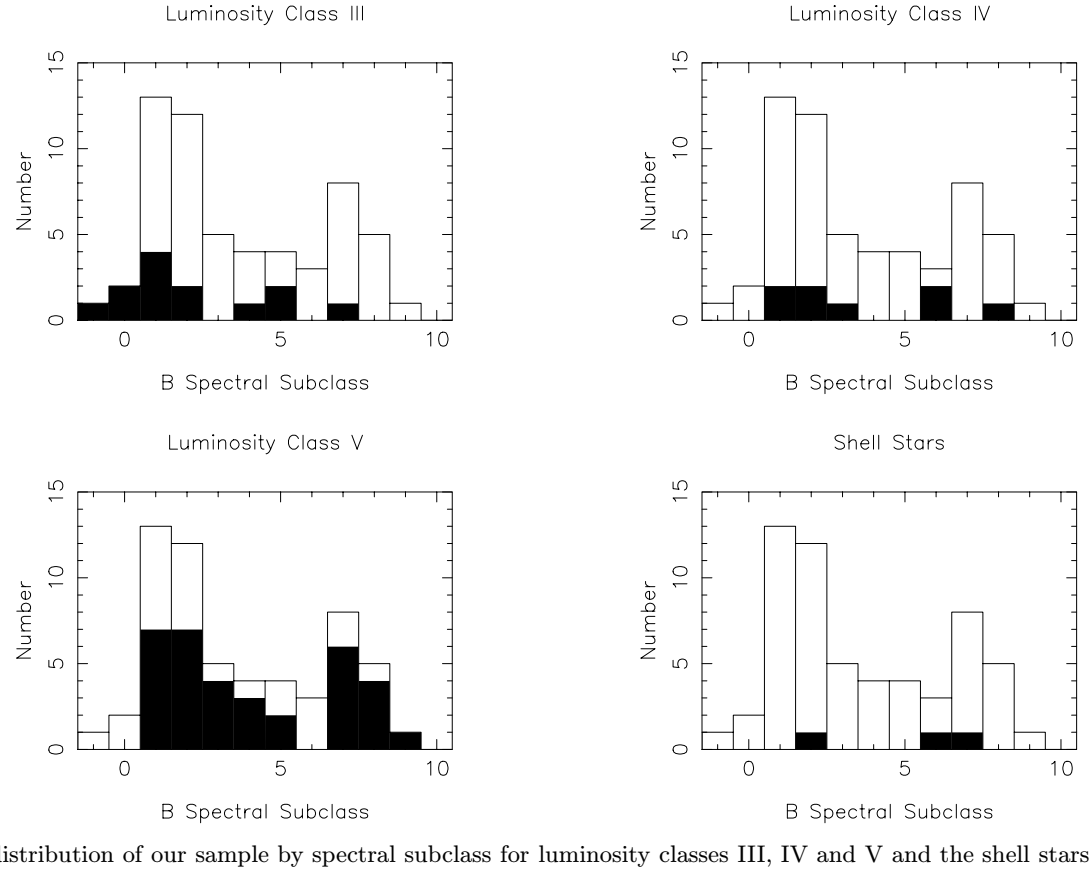

Fig. 5. The distribution of our sample by spectral subclass for luminosity classes III, IV and V and the shell stars (solid area). Also plotted on each histogram (hollow area) is the overall distribution neglecting luminosity class. The data have been binned into bins n containing objects in the range range B(n-1).5 to B(n).4. Therefore a B0.2 object will appear in the B0 bin, however a B0.5 object appears in the B1 bin

certainly within the range B0.5III – B1III and both B0.5III and B1III look inadequate classifications. The luminosity classification is also secure in this range, where we are able to differentiate clearly between giants and main sequence objects.

4.3. Late B stars

For stars later than B5, all the classification criteria available are strongly affected by the presence of an emission continuum. This has resulted in our determinations for this spectral range being slightly less secure than for earlier spectral types. However, with few exceptions, we have been able to assign a spectral type to the correct subtype. This means that we feel that a star classified as B6V would be inadequately classified as B5 or B7. The luminosity classification is slightly less certain. For this reason, we have resorted to using two extra criteria, namely, the number of Balmer lines that could be resolved in the spectrum as it approaches the Balmer discontinuity and the full width half maximum of Hθ (3797 Å), which, among the standard stars, correlates strongly with luminosity class at a given spectral type and is not generally affected by emission in the Be stars. Overall, the three methods do not show strong discrepancies and our luminosity classification can be considered secure, at least to the point of discriminating between giant and main sequence stars.

Lesh (1968) defines B8V by the condition Mg II λ4481 Å $\simeq$ He I λ4471 Å. However, as can be seen in Fig. 4, the spectrum of HD 214923 (ζ Peg), given by Jaschek & Gómez (1998) as B8V standard, shows the Mg II line to be clearly stronger than the He I line. Therefore, this object must be of a later spectral type. Comparison with HD 196867 (α Del) shows that this object is not later than B9V. We have taken the spectral type of this object to be B9V, though we believe that B8.5V could be an adequate interpolation. No object in our sample is so late as HD 214923 and therefore we assign to BD +55°2411, the only object in the sample with Mg II λ4481 Å clearly stronger than He I λ4471 Å a spectral type B8.5V.

In the spectral region B7-B8, where the ratio between Mg II λ4481 Å and He I λ4471 Å is the only classification criteria, in-filling can strongly affect the derived spectra. For that reason, we have also used the strength of the Si II doublet and of the whole He I spectrum as additional information. Moreover, at this resolution, C II λ4267 Å is visible in main sequence stars up to spectral type B7V. Fe II λ4232 Å starts to be visible in the B8V spectra, but we have not used it as a classification indicator since it can also be a weak shell line.

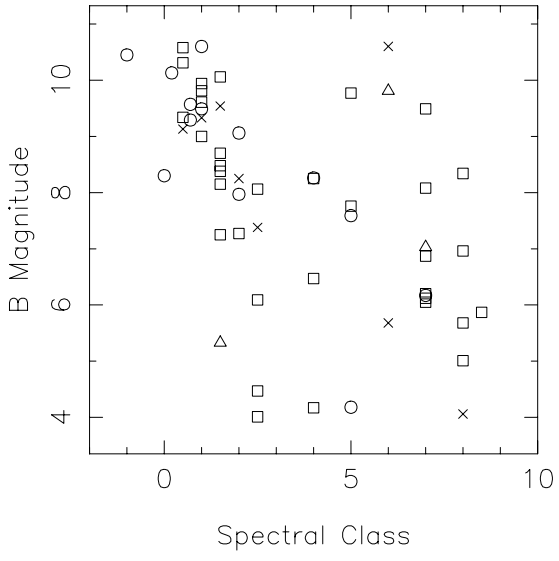

Fig. 6. Apparent B magnitude versus B spectral subclass for the sample. Luminosity class is indicated by the symbols, where a circle indicates III, a cross IV and a square V. Objects with a shell spectrum are indicated by the triangles

4.4. Shell stars

For the purpose of spectral classification, we have only marked as "shell" stars those showing narrow absorption Fe II lines, either on top of emission lines or blanketing the continuum. Several other stars show double-peaked emission split by an absorption core in some Balmer lines, but this emission is still inside the photospheric absorption feature and does not reach the continuum (e.g., BD +37 675 and BD +42 1376 in Fig. 1). The shell definition is not applicable since no iron lines are visible (see Hanuschik 1995). Exceptions could be BD +47 857 and BD +50 3430 which seem to show absorption cores in some Fe II emission lines and therefore could be shell stars. We will revisit this question in future papers when we discuss the emission line spectra of the objects.

4.5. Distribution of spectral types within the sample

In Fig. 5 we plot histograms showing the total number of objects of each spectral type and luminosity class in our sample. For the purposes of the histograms and the discussion that follows we have classified the two early objects we give luminosity class II as III, and the objects we classify as "III-V" as IV. Apart from the very earliest objects, which are all giants, the distributions of objects between the three luminosity classes with respect to spectral type are similar. This is probably a selection effect in that there are very few early-type stars, so most are far away and our magnitude limited sample only selects the more luminous giants. From Fig. 6 we note that these very early objects are near the magnitude limit of our sample, thus supporting this interpretation.

Table 4. Measured Spectral Type and $v \sin i$ for the Be star sample

OBJECT	Spec. type	$v \sin i$
CD −28 14778	B2III	153 ± 21
CD −27 11872	B0.5V-III	224 ± 33
CD −27 16010	B8IV	187 ± 32
CD −25 12642	B0.7III	77 ± 18
CD −22 13183	B7V	174 ± 10
BD −20 05381	B5V	202 ± 10
BD −19 05036	B4III	121 ± 10
BD −12 05132	BN0.2III	120 ± 43
BD −02 05328	B7V	151 ± 15
BD −01 03834	B2IV	168 ± 34
BD −00 03543	B7V	271 ± 54
BD +02 03815	B7-8shell	224 ± 14
BD +05 03704	B2.5V	221 ± 10
BD +17 04087	B6III-V	156 ± 39
BD +19 00578	B8V	240 ± 70
BD +20 04449	B0III	81 ± 11
BD +21 04695	B6III-V	146 ± 10
BD +23 01148	B2III	101 ± 10
BD +25 04083	B0.7III-B1II	79 ± 11
BD +27 00797	B0.5V	148 ± 74
BD +27 00850	B1.5IV	112 ± 25
BD +27 03411	B8V	194 ± 10
BD +28 03598	O9II	90 ± 12
BD +29 03842	B1II	91 ± 16
BD +29 04453	B1.5V	317 ± 20
BD +30 03227	B4V	218 ± 21
BD +31 04018	B1.5V	211 ± 11
BD +36 03946	B1V	186 ± 21
BD +37 00675	B7V	207 ± 29
BD +37 03856	B0.5V	104 ± 17
BD +40 01213	B2.5IV	128 ± 20
BD +42 01376	B2V	196 ± 10
BD +42 04538	B2.5V	282 ± 10
BD +43 01048	B6IIIshell	220 ± 20
BD +45 00933	B1.5V	148 ± 16
BD +45 03879	B1.5V	193 ± 10
BD +46 00275	B5III	113 ± 21
BD +47 00183	B2.5V	173 ± 12
BD +47 00857	B4V-IV	212 ± 16
BD +47 00939	B2.5V	163 ± 12
BD +47 03985	B1-2shell	284 ± 20
BD +49 00614	B5III	90 ± 27
BD +50 00825	B7V	187 ± 10
BD +50 03430	B8V	230 ± 15
BD +51 03091	B7III	106 ± 10
BD +53 02599	B8V	191 ± 23
BD +55 00552	B4V	292 ± 17
BD +55 00605	B1V	126 ± 35
BD +55 02411	B8.5V	159 ± 90
BD +56 00473	B1V-III	238 ± 19
BD +56 00478	B1.5V	157 ± 12
BD +56 00484	B1V	173 ± 16
BD +56 00493	B1V-IV	270 ± 10
BD +56 00511	B1III	99 ± 14
BD +56 00573	B1.5V	250 ± 58
BD +57 00681	B0.5V	147 ± 49
BD +58 00554	B7V	229 ± 10
BD +58 02320	B2V	243 ± 20

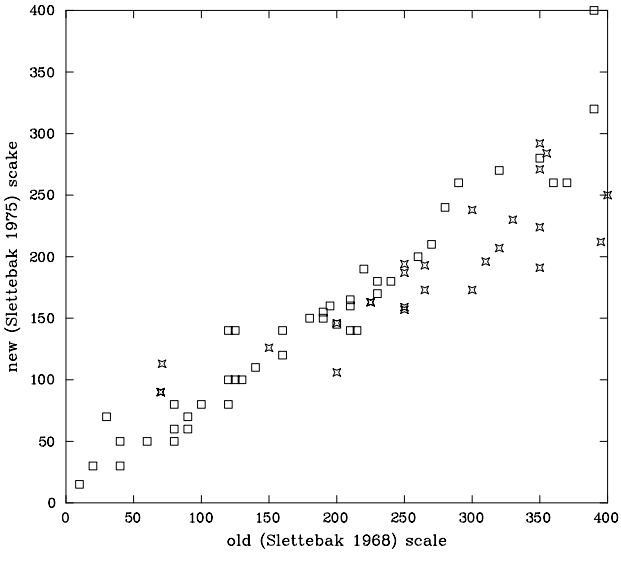

Fig. 7. Comparison of "old" (Slettebak 1968) and "new" (Slettebak 1975) $v \sin i$ scales for B stars (square symbols) and our measurements of Be stars (new scale) versus Bernacca & Perinottot's (1970, 1971) (old scale) data for the same objects (star symbols)

Considering the sample as a whole it is interesting to note the majority (34 out of 58) objects are dwarfs, with only 13 out of 58 unambiguously classified as giants. Recall that in Sect. 2 our selection criteria were designed to give an equal number of these objects. This implies that in spectral types given by Jaschek & Egret (1982) many objects that are classified as luminosity class III should in fact be classified as IV or V. In this case it is unlikely that this is a bias created by our selection of objects from the catalogue, as our magnitude limit would be expected to select the more luminous giants over the dwarfs.

5. Rotational velocities

5.1. Methodology

In order to derive rotational velocities we attempted to fit Gaussian profiles to 4 HeI lines at 4026 Å, 4143 Å, 4387 Å and 4471 Å in the spectra. This was successful for most of the objects, although for a small number only 2 or 3 lines could be reliably fitted due to contamination by nearby emission or absorption features. The profile full widths at half maximum were converted to $v \sin i$ using a fit to the 4471 Å full width half maximum - $v \sin i$ correlation of Slettebak et al. (1975). Making the appropriate correction for the differing central wavelengths of each line, the fits employed were:

$$v \sin i = 41.25F(4471) \text{ km s}^{-1} \quad (1)$$

$$v \sin i = 42.03F(4387) \text{ km s}^{-1} \quad (2)$$

$$v \sin i = 44.51F(4143) \text{ km s}^{-1} \quad (3)$$

$$v \sin i = 45.82 F(4026) \text{ km s}^{-1} \quad (4)$$

where $F(\lambda)$ is the full width half maximum in Å at a wavelength of λ Å. The $v \sin i$ quoted in Table 4 is the mean of those derived from all of the fitted lines for each object after correction for the mean instrumental velocity dispersion of 55 km s^{-1} (determined from measurements of interstellar lines in the spectra). The errors reflect the dispersion in the measured full width half maxima, with the minimum error set at 10 km s^{-1}.

26 of the objects in our sample have previously measured $v \sin i$'s in the compilations of Bernacca & Perinotto (1970, 1971). A comparison of the historical $v \sin i$'s with those we derive shows the historical values typically ~ 20 per-cent greater than our values. However Bernacca & Perinotto (1974) state that their $v \sin i$'s are referenced to the scale of Slettebak (1968) whereas our measurements are instead referenced to Slettebak et al. (1975). Figure 7 of that paper shows that the new (1975) scale derives $v \sin i$'s some $15 - 20$ per-cent smaller for B stars than the old (1968) scale and so the discrepancy may simply be understood to be caused by our use of a more modern $v \sin i$ calibration. To make this clear Fig. 7 replots Fig. 7 of Slettebak et al. (1975) with their standard stars marked as squares and our sample marked as crosses. No significant difference is apparent between the two distributions.

5.2. Distribution of rotational velocities within the sample

In Fig. 8 (hollow plus filled areas) we plot the distribution of $v \sin i$ versus spectral type within the sample for luminosity classes III, IV and V. It is important to identify whether there are are biases in the $v \sin i$ values within the sample. There are two effects that may lead to a relationship between $v \sin i$ and brightness for Be stars and in a flux limited sample we would of course expect an inherent bias towards intrinsically brighter objects.

The first effect that would lead to a bias towards rapidly rotating Be stars is described by Zorec & Briot (1997). The more rapidly rotating stars will suffer greater deformation than the slower rotators. Although the bolometric luminosity from an object is of course conserved, the effect of rotation is to make the spectrum appear cooler. Since the peak of B star spectra is in the UV, this will make the optical flux brighter for most aspect ratios (Collins et al. 1991; Porter 1995), leading to the preferential selection of more rapidly rotating stars in a magnitude limited sample.

In addition it is well known that the emission produced in the circumstellar envelope of Be stars leads to an increase in their optical flux. Observations of phase changes from non-Be to Be typically show increases of $0.1 - 0.2$ magnitudes (Feinstein 1975; Apparao 1991). This is due to reprocessing of the UV radiation from the underlying Be star into optical and infrared light by the disk. Assuming a relation between disk size and excess optical flux we would therefore expect stars with larger circumstellar disks to be preferentially selected by our flux limited sample. Also assuming that the sizes of Be star disks are likely to be sensitive to the stellar rotational velocity, then we would expect the most rapidly rotating stars to show the strongest optical excess. This again would lead to a bias towards rapidly rotating Be stars in a magnitude limited sample.

In order to test whether our sample is biased in this way we must compare it to a volume limited subset. This can be created from our sample by using the absolute magnitudes (Schmidt-Kaler 1982) derived from the spectral and luminosity classes to select objects that lie within the volume defined by the absolute magnitude limit for

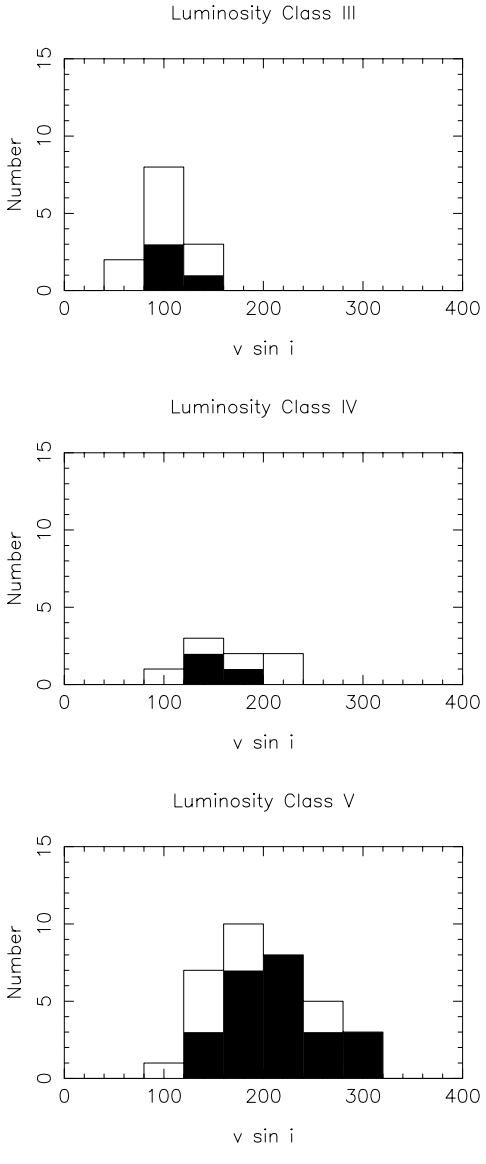

Fig. 8. $v \sin i$ distributions for all objects in the sample (hollow plus filled areas) and objects in a volume limited subset of the sample (filled area only)

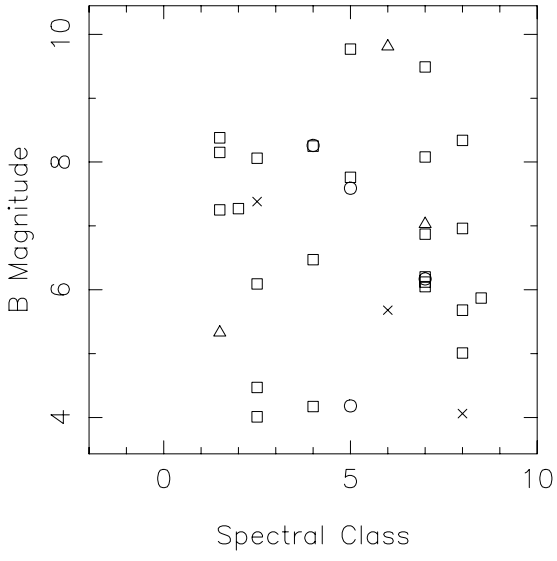

Fig. 9. Apparent B magnitude versus B spectral subclass for the volume limited sample. Symbols as per Fig. 6

the intrinsically faintest objects (B9V) at the apparent magnitude limit ($B \sim 11$). The resulting volume limited subsample contains 34 objects out of our original 58. We plot the B magnitude distribution of this subsample in Fig. 9. Note how the volume limiting naturally cuts out the objects with faint apparent magnitudes at early spectral types (cf. Fig. 6). The $v \sin i$ distribution of the volume limited subsample is plotted in Fig. 8 (filled area only) to allow comparison with the total sample (filled plus hollow area). In order to compare the distributions we use a Kolmogorov-Smirnov (KS) test between the volume-limited and total samples. This shows that the probability of the distribution of $v \sin i$ two samples being the same is 80% for luminosity class III, 99% for luminosity class IV, and 95% for luminosity class V. There is therefore no statistical evidence for any bias in the $v \sin i$ values for all three luminosity classes in the sample. What is clear from Fig. 8 is that there is a considerably lower mean $v \sin i$ for luminosity class III as opposed to class V Be stars. The astrophysical interpretation of this result is discussed in Steele (1999).

6. Conclusions

We have selected a sample of 58 Be stars of spectral types O9 to B8.5 and luminosity classes III to V. We have classified the spectra by comparison with standards observed at the same time and derived $v \sin i$ values by measuring the $FWHM$ of 4 HeI lines. Although our initial criteria were designed to select equal numbers of dwarfs and giants, in fact our sample is dominated by dwarfs. The few giants within the sample tend to have lower rotational velocities than the dwarfs. By comparison with a volume limited subsample we have shown that this is not a selection effect.

The sample defined in this paper has also been observed at other optical and infrared wavelengths. The results of those observations will be presented in future papers, where the line emission detected will be used in an attempt to correlate the properties of the circumstellar disk with those derived in this paper.

Acknowledgements. This research has made use of the SIMBAD database of the CDS, Strasbourg. The Isaac Newton Telescope is operated on the Island of La Palma by the Isaac Newton Group in the Spanish Observatorio del Roque de los Muchachos of the Instituto de Astrofisica de Canarias. IN and JSC were supported by PPARC.

References

Apparao K.M.V., 1991, ApJ 376, 256
Bernacca P.L., Perinotto M., 1970, Contr. Oss. Astrof. Asiago, 239
Bernacca P.L., Perinotto M., 1971, Contr. Oss. Astrof. Asiago, 250
Bernacca P.L., Perinotto M., 1974, A&A 33, 443
Collins II G.W., Truax R.J., Cranmer S.R., 1991, ApJS 77, 541
Dachs J., Poetzel R., Kaiser D., 1989, A&AS 78, 487
Feinstein A., 1975, PASP 87, 603
Hanuschik R.W., 1995, A&A 295, 423
Jaschek C., Gómez A.E., 1998, A&A 330, 619
Jaschek M., Egret D., 1982, Proc. IAU Symp. 98, 261 (Knudsen)
Lesh J.R., 1968, ApJS 16, 371
Morgan W.W., Keenan P.C., 1973, ARA&A 11, 29
Porter J.M., 1995, PhD Thesis, Univ. Oxford
Schmidt-Kalter Th., 1982, in: Landolt Bornstein New Series, Vol. 2b, Schaifers K., Voight H.H. (eds). Springer Verlag, Berlin
Slettebak A., 1968, ApJ 151, 1043
Slettebak A., Collins G.W., Boyce P.B., White N.M., Parkinson T.D., 1975, ApJS 281, 137
Steele I.A., 1999, A&A 343, 237
Walborn N.R., 1971, ApJS 23, 257
Walborn N.R., 1973, AJ 78, 1067
Zorec J., Briot D., 1997, A&A 318, 443